Giant all-optical tunable group velocity dispersion in an optical fiber

Yunhui Zhu,[1,2] Joel A. Greenberg,[1,3] Nor Ain Husein,[1,4] and Daniel J. Gauthier[1,*]

[1]*Department of Physics and Fitzpatrick Institute for Photonics, Box 90305, Duke University, Department of Physics, Durham, North Carolina 27708, USA*

[2]*Currently with Massachusetts Institute of Technology, Department of Mechanical Engineering, Room 3-466, 77 Massachusetts Ave., Cambridge MA 02139, USA*

[3]*Currently with Department of Electrical and Computer Engineering and Fitzpatrick Institute for Photonics, Box 90291, Duke University, Durham, North Carolina 27708, USA*

[4]*Currently with Advanced Photonic Science Institute, Universiti Teknologi Malaysia, UTM Johor Bahru, 81310, Johor, Malaysia*

[*]*gauthier@phy.duke.edu*

Abstract: We realize a strongly dispersive material with large tunable group velocity dispersion (GVD) in a commercially-available photonic crystal fiber. Specifically, we pump the fiber with a two-frequency pump field that induces an absorbing resonance adjacent to an amplifying resonance via the stimulated Brillouin processes. We demonstrate all-optical control of the GVD by measuring the linear frequency chirp impressed on a 28-nanosecond-duration optical pulse by the medium and find that it is tunable over the range ± 7.8 ns^2/m. The maximum observed value of the GVD is 10^9 times larger than that in a typical single-mode silica optical fiber. Our observations are in good agreement with a theoretical model of the process.

OCIS codes: (260.2030) Dispersion; (130.2035) Dispersion compensation devices; (190.4370) Nonlinear optics, fibers; (290.5900) Scattering, stimulated Brillouin.

References and links

1. J. B. Pendry, D. Schurig, and D. R. Smith, "Controlling electromagnetic fields," Science **312**(5781), 1780–1782 (2006).
2. R. W. Boyd and D. J. Gauthier, "Controlling the Velocity of Light Pulses," Science **326**(5956), 1074–1077 (2009).
3. A. M. Weiner, *Ultrafast optics* (John Wiley and Sons, New Jersey, 2009).
4. J. Mower, Z. Zhang, P. Desjardins, C. Lee, J. H. Shapiro, and D. Englund, "High-dimensional quantum key distribution using dispersive optics," Phys. Rev. A **87**(6), 062322 (2013).
5. J. Nunn, L. J. Wright, C. Söller, L. I. Zhang, I. A. Walmsley, and B. J. Smith, "Large-alphabet time-frequency entangled quantum key distribution by means of time-to-frequency conversion," Opt. Express **21**(13), 15959–15973 (2013).
6. J. M. Donohue, M. Agnew, J. Lavoie, and K. J. Resch, "Coherent Ultrafast Measurement of Time-Bin Encoded Photons," Phys. Rev. Lett. **111**(15), 153602 (2013).
7. J. P. Yao, "A tutorial on microwave photonics - Part I," IEEE Photon. Soc. Newsletter **26**, 4–12 (2012).
8. P. Bowlan and R. Trebino, "Complete single-shot measurement of arbitrary nanosecond laser pulses in time," Opt. Express **19**(2), 1367–1377 (2011).
9. M. Fridman, A. Farsi, Y. Okawachi, and A. L. Gaeta, "Demonstration of temporal cloaking," Nature **481**(7379), 62–65 (2012).
10. L. V. Hau, S. E. Harris, Z. Dutton, and C. H. Behroozi, "Light speed reduction to 17 meters per second in an ultracold atomic gas," Nature **397**(6720), 594–598 (1999).
11. Y. Okawachi, M. S. Bigelow, J. E. Sharping, Z. Zhu, A. Schweinsberg, D. J. Gauthier, R. W. Boyd, and A. L. Gaeta, "Tunable all-optical delays via Brillouin slow light in an optical fiber," Phys. Rev. Lett. **94**(15), 153902 (2005).
12. K. Y. Song, M. G. Herráez, and L. Thévenaz, "Observation of pulse delaying and advancement in optical fibers using stimulated Brillouin scattering," Opt. Express **13**(1), 82–88 (2005).
13. G. P. Agrawal, *Nonlinear Fiber Optics*, 3rd Ed. (Academic Press, San Diego, 2001), Chs. 1–4.
14. M. D. Stenner, M. A. Neifeld, Z. Zhu, A. M. C. Dawes, and D. J. Gauthier, "Distortion management in slow-light pulse delay," Opt. Express **13**(25), 9995–10002 (2005).

#210131 - $15.00 USD Received 14 Apr 2014; revised 27 May 2014; accepted 29 May 2014; published 4 Jun 2014

15. Y. Wu, L. Zhan, Y. Wang, S. Luo, and Y. Xia, "Low distortion pulse delay using SBS slow- and fast-light propagation in cascaded optical fibers," J. Opt. Soc. Am. B **28**(11), 2605–2610 (2011).
16. R. W. Boyd, *Nonlinear Optics*, 3rd Ed. (Academic Press, Amsterdam, 2008), Ch. 9.
17. M. Born and E. Wolf, *Principles of Optics*, 7th Ed. (Cambridge University, Cambridge, 2002), Ch. II.
18. Y. Zhu, M. Lee, M. A. Neifeld, and D. J. Gauthier, "High-fidelity, broadband stimulated-Brillouin-scattering-based slow light using fast noise modulation," Opt. Express **19**(2), 687–697 (2011).
19. Z. Zhu, A. M. C. Dawes, D. J. Gauthier, L. Zhang, and A. E. Willner, "Broadband SBS slow light in an optical fiber," J. Lightwave Technol. **25**(1), 201–206 (2007).
20. K. Y. Song and K. Hotate, "25 GHz bandwidth Brillouin slow light in optical fibers," Opt. Lett. **32**(3), 217–219 (2007).
21. R. Pant, C. G. Poulton, D.-Y. Choi, H. Mcfarlane, S. Hile, E. Li, L. Thevenaz, B. Luther-Davies, S. J. Madden, and B. J. Eggleton, "On-chip stimulated Brillouin scattering," Opt. Express **19**(9), 8285–8290 (2011).
22. H. Shin, W. Qiu, R. Jarecki, J. A. Cox, R. H. Olsson 3rd, A. Starbuck, Z. Wang, and P. T. Rakich, "Tailorable stimulated Brillouin scattering in nanoscale silicon waveguides," Nat. Commun. **4**, 1944 (2013).
23. G. Bahl, K. H. Kim, W. Lee, J. Liu, X. Fan, and T. Carmon, "Brillouin cavity optomechanics with microfluidic devices," Nat. Commun. **4**, 1994 (2013).
24. Y. Zhu, J. Kim, and D. J. Gauthier, "Aberration-corrected quantum temporal imaging," Phys. Rev. A **87**(4), 043808 (2013).
25. M. Aspelmeyer, P. Meystre, and K. Schwab, "Quantum Optomechanics," Phys. Today **65**(7), 29–35 (2012).
26. J. A. Greenberg and D. J. Gauthier, "Transient dynamics and momentum redistribution in cold atoms via recoil-induced resonances," Phys. Rev. A **79**(3), 033414 (2009).
27. S. P. Shipman and S. Venakides, "Resonant transmission near nonrobust periodic slab modes," Phys. Rev. E Stat. Nonlin. Soft Matter Phys. **71**(2), 026611 (2005).
28. S. H. Mousavi, I. Kholmanov, K. B. Alici, D. Purtseladze, N. Arju, K. Tatar, D. Y. Fozdar, J. W. Suk, Y. Hao, A. B. Khanikaev, R. S. Ruoff, and G. Shvets, "Inductive tuning of Fano-resonant metasurfaces using plasmonic response of graphene in the mid-infrared," Nano Lett. **13**(3), 1111–1117 (2013).
29. R. Singh, I. A. I. Al-Naib, M. Koch, and W. Zhang, "Sharp Fano resonances in THz metamaterials," Opt. Express **19**(7), 6312–6319 (2011).

1. Introduction

Breakthrough research over the past decade has demonstrated unprecedented control over the frequency-dependent refractive index of optical materials. For example, it is now possible to obtain negative values of the refractive index [1] using metamaterials and extremely large or negative values of the group index using laser-induced material resonances or photonic crystals [2]. In contrast, engineering the group velocity dispersion (GVD) is limited to the domain of ultra-fast light pulses [3], and therefore relies heavily on complicated and specified devices for picosecond or sub picosecond laser pulse generation. Yet, emerging applications, such as quantum key distribution [4,5], quantum [6] and classical [7,8] information processing, and temporal cloaking [9] require or can benefit from large GVD that can disperse longer-duration pulses. In these applications to date, optical pulse durations are typically in the sub-nanosecond regime for classical and quantum optical fiber telecommunication [6–8]. On the other hand, the photonic wavepackets that are used to convey qubits between quantum dots can have lifetimes on the order of several nanoseconds [6]. A large tunable dispersive element would immediately benefit passive dispersion compensation control, and moreover, enable the application of temporal Fourier operations into these emerging fields.

Motivated by recent research [10–12] that has demonstrated extreme values of group index using resonances to enhance the material dispersion, we find that giant values of the GVD parameter β_2 can be obtained when an amplifying resonance is placed next to an absorbing resonance. Here, we demonstrate giant and adjustable GVD over the range ± 7.8 ns^2/m appropriate for nanosecond-duration pulses realized using an optical fiber pumped by an auxiliary laser beam. The dispersion is ~10^9 times larger than that obtained in standard single-mode fiber. This method can be used for any wavelength within the transparent window of the optical fiber. In addition, the GVD dispersion value is widely tunable and the spectral profile can be optimized for specific applications by tailoring the pump-laser spectrum. The unprecedented large GVD value and wide tunability are promising avenues for applications involving the dispersion of long-duration pulses.

#210131 - $15.00 USD Received 14 Apr 2014; revised 27 May 2014; accepted 29 May 2014; published 4 Jun 2014

2. Theory of group velocity dispersion design

In general terms, our approach can be understood by considering one-dimensional pulse propagation along the *z*-direction in a linear dispersive material characterized by a frequency-dependent complex refractive index *n(ω)*. In this case, electromagnetic theory predicts that the spectral amplitude of the output field is related to its input through the relation

$$E_{out}(\omega) = e^{i\beta(\omega)z} E_{in}(\omega) \tag{1}$$

where $\beta(\omega) = n(\omega)\omega / c$ is the pulse complex wavevector in the dispersive material and c is the speed of light in vacuum [13].

For pulses with a narrow-band spectrum centered at the carrier frequency ω_0 and slow variation of $n(\omega)$ over the pulse spectrum, a Taylor series expansion of the complex wavevector

$$\beta(\omega) = \beta_0(\omega_0) + \beta_1(\omega - \omega_0) + \beta_2(\omega - \omega_0)^2 / 2! + \beta_3(\omega - \omega_0)^3 / 3! + \cdots \tag{2}$$

leads to approximate analytic solutions to the problem when the series is truncated, where the complex dispersion parameters are defined by $\beta_j = d^j \beta / d\omega^j \big|_{\omega=\omega_0}$. For the case when β is essentially real, as appropriate for transparent glasses, the phase velocity of the pulse is given by $v_p = c / n(\omega_0) = \omega_0 / \beta_0$, and the group velocity is $v_g = c / n_g = 1 / \beta_1$. For slow- and fast-light applications, the goal is to design a material that has large or small n_g (β_1) and to minimize the higher-order dispersion terms ($j > 1$) [14,15]. On the other hand, for a material dominated by GVD, the goal is to design a material with large $|\beta_2|$ and to minimize the other terms in Eq. (2).

For a material dominated by GVD, an incident transformed-limited pulse develops a linear frequency chirp (corresponding to a quadratic phase), as illustrated in Fig. 1(a). The characteristic distance over which the chirp develops is known as the dispersion length $L_D = \tau_0^2 / |\beta_2|$, where τ_0 is a measure of the pulse width. The substantial dispersion needed for the applications mentioned above requires that the length of the material $L \sim L_D$. The scaling of L_D with pulse width is the reason why it is difficult to observe GVD-effects for nanosecond-duration pulses for values of β_2 characteristic of typical dispersive materials and devices (for example, β_2 ~20 ps^2/km for single-mode silica optical fibers at 1.55 μm).

As mentioned above, we engineer a material with large GVD by considering the dispersion resulting from two neighboring resonances. The linear optical susceptibility for such a composite resonance, consisting of the case of a Lorentzian-shaped amplifying resonance at frequency $\omega_r - \Delta$, half-width γ, and strength G>0 and a similar absorbing resonance at frequency $\omega_r + \Delta$ and strength -G, is given by

$$\chi(\omega) = i \frac{c n_h G}{\omega_r} \left[-\frac{1}{1 - i(\delta + \Delta)/\gamma} + \frac{1}{1 - i(\delta - \Delta)/\gamma} \right]. \tag{3}$$

Here, the first (second) term in Eq. (3) represents the amplifying (absorbing) resonance, ω_r is the center of the composite resonance, $\delta = \omega - \omega_r$ is the detuning relative to the center of the resonance, 2Δ is the frequency separation between the gain and absorption line, n_h is the index of refraction of the transparent host material and $n(\omega) \cong n_h + \chi(\omega) / 2n_h$, which is valid when the resonance is not too strong so that local-field effects can be ignored. The GVD parameter arising from the resonance profile described by Eq. (3) is obtained by taking the

#210131 - $15.00 USD Received 14 Apr 2014; revised 27 May 2014; accepted 29 May 2014; published 4 Jun 2014

Taylor-series expansion of this expression. We find that the GVD value at the central frequency $\delta = 0$ is given by

$$\beta_2 = \frac{G}{\gamma^2}\left(\frac{2\tilde{\Delta}(-3+\tilde{\Delta}^2)}{(1+\tilde{\Delta}^2)^3}\right), \tag{4}$$

with $\tilde{\Delta} \equiv \Delta/\gamma$.

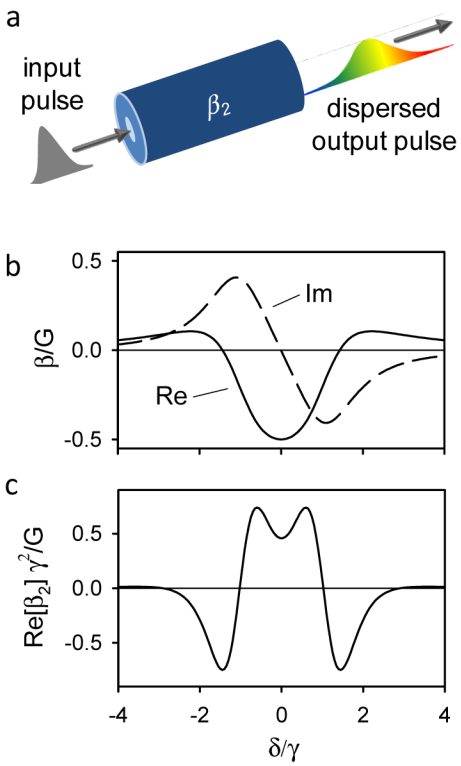

Fig. 1. Group velocity dispersion in optical material. a An input transform-limited optical pulse develops a linear frequency chirp as it propagates through a material with group velocity dispersion parameter β_2 (illustrated here for the case when $\beta_2 > 0$). b Wavevector magnitude for a medium containing oscillators with a double resonance described by the susceptibility given by Eq. (3) with $\Delta/\gamma = -1.03$. c GVD parameter for the double-resonance medium for the same conditions as in b.

Figure 1(b) shows the complex wavevector profile for the susceptibility given by Eq. (3). It is seen that the real part of β is symmetric about $\delta = 0$, as opposed to anti-symmetric for a single Lorentzian resonance, which gives rise to large slow- and fast-light effects. In addition β is approximately quadratic about $\delta = 0$, which results in large positive β_2 given by Eq. (4), as shown in Fig. 1(c). The profiles are inverted by changing the sign of Δ, which allows easy control over the sign of the GVD. The magnitude of the GVD value is controlled by the gain G.

3. Experimental realization and measurement of giant tunable GVD in a photonic crystal fiber

The dispersion profile in Fig. 1(b) is realized experimentally by inducing stimulated Brillouin scattering (SBS) resonances in a 10-meter-long photonic crystal optical fiber. The experimental setup used to observe large GVD is shown in Fig. 2. In the typical SBS process,

#210131 - $15.00 USD Received 14 Apr 2014; revised 27 May 2014; accepted 29 May 2014; published 4 Jun 2014

a weak input laser beam interacts with a strong counterpropagating pump beam through wave mixing with an induced acoustic field [16], creating narrow Stokes (amplifying) and anti-Stokes (absorbing) resonances whose strengths are proportional to the pump beam intensity. SBS resonances can be induced at any frequency where the material is transparent by adjusting the pump laser frequency, thus making this approach broadly tunable over the entire transparency window of the fiber (limited only by the availability of the laser source). To obtain adjacent amplifying and absorbing resonances as required by Eq. (3), we pump the PCF using a two-frequency pump beam that allows us to place the anti-Stokes resonance arising from one of the pump frequency components close to the Stokes resonance arising from the other component, as illustrated in Fig. 3(a).

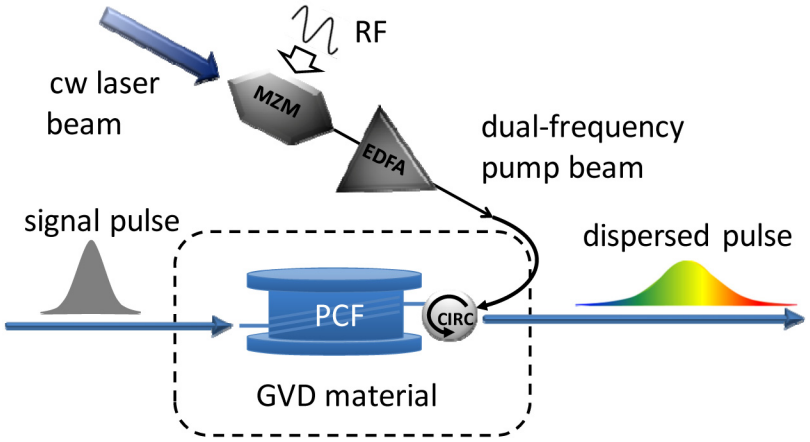

Fig. 2. Schematic of the experimental setup to observe giant GVD. We use a 10-m-long PCF (NKT Photonics Inc., NL-1550-NEG-1, SBS gain factor g_{SBS} = 2.5 ± 0.2 $W^{-1}m^{-1}$, SBS resonance width $\gamma/2\pi$ = 23.8 ± 0.6 MHz, and Brillouin frequency $\Omega_B/2\pi$ = 9.60 GHz) that is pumped by a 1.55-μm-wavelength bichromatic pump beam. The pump beam is created by modulating the output of a telecommunications laser (Fitel 47X97A04) with a Mach-Zehnder modulator (EOSpace, AX-0K1-12-PFAP-PFA-R3-UL, 20 GHz) operating in carrier-suppression mode and driven by a sinusoidal waveform at frequency produced by a microwave frequency source (Agilent E8267D). The modulated pump beam is passed through an erbium-doped fiber amplifier (IPG Photonics EAD-1K) and a Faraday circulator before injection into the PCF so that it counterpropagates with respect to the signal beam. It is noted that such an experiment setting is not mandatory to realize giant GVD; we can also use two laser diodes as the dual-frequency pump given that the frequency jitter is small and stable.

As a first step in characterizing the dispersive material, we inject a weak continuous-wave signal beam into the bichromatically-driven PCF and measure the gain spectrum of the composite SBS resonances as shown in Fig. 3(b). We use an auxiliary signal laser beam (Agilent HP81862A, power 3.6 μW,) whose frequency is scanned via current tuning. This beam is passed through a circulator before injection into the PCF. The signal beam is passed to a photoreceiver (New Focus 1611) via the other circulator and measured with an oscilloscope. When $\Delta = 0$, there is essentially no change in the transmitted signal beam, demonstrating that the Stokes and anti-Stokes resonances do not depend on the relative phases of the pump beam frequency components and hence the susceptibility given by Eq. (3) is appropriate. When $\Delta < 0$, we obtain a gain profile corresponding to the imaginary part of β shown in Fig. 1(b). The profile inverts, as discussed above, when $\Delta > 0$.

We next inject nanosecond-scale-duration, chirp-free Gaussian-shaped signal pulses with $\omega_0 = \omega_r$ into the PCF and measure the frequency chirp using a homodyne detection technique that mixes some of the continuous wave pump laser light (serving as a phase reference) with the pulse transmitted (power $P_{out}(t)$) from the PCF. For the pulsed experiments, we generate

#210131 - $15.00 USD Received 14 Apr 2014; revised 27 May 2014; accepted 29 May 2014; published 4 Jun 2014

the signal beam by splitting a small fraction of the power from the pump beam, thereby assuring that $\omega_0 = \omega_r$. This beam is passed through a Mach-Zehnder modulator (OTI 10 Gb/s) driven by an arbitrary waveform generator (Tektronix AFG 3251) that generates a Gaussian-like pulse of the form $P(t) = P_0 \exp[-(t/\tau_0)^2]$, where P_0 is the peak power and τ_0 = 28.0 ns.

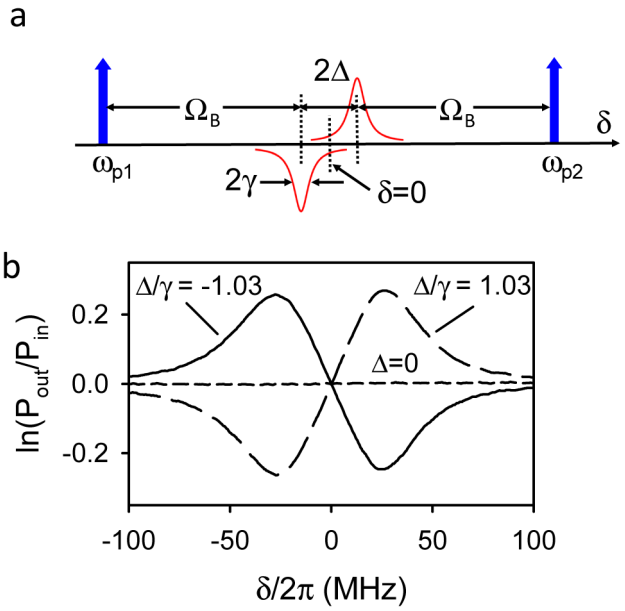

Fig. 3. Composite SBS resonance. a Illustration of SBS resonances. A counterpropagating pump beam of frequency ω_{p1} induces an anti-Stokes absorption line at frequency $\omega_{p1} + \Omega_B$ and full-width at half-maximum width 2γ, and the pump beam component at frequency ω_{p2} induces a Stokes gain line at frequency $\omega_{p2} - \Omega_B$, also with the same width. These induced resonances are shown in red. The strength of the resonances are identical in magnitude and given by $G = g_{SBS} P_{pj}$, where g_{SBS} is the SBS gain factor and P_{pj} is the pump power of the pump beam at frequency j (= 1, 2). The center of the composite SBS resonance is at frequency ω_r and the frequency relative to this value is denoted by δ. The spacing between the gain and absorption lines is 2Δ, shown here for the case when $\Delta > 0$. b Experimentally observed probe beam transmission profile for different values of Δ, showing the natural logarithm of the output probe beam power P_{out} divided by the input power P_{in} with $GL = 0.33 \pm 0.03$.

As shown in Fig. 4(a), with the reference blocked (Fig. 1(a)), we observe the broadened Gaussian shaped profile of the pulse. With the reference unblocked, the profile displays interference due to the frequency chirp, which agrees well with the expected dependence. We repeat this measurement for different pump powers and hence SBS gain G. The waveform is captured with an 8-GHz-analog-bandwidth, 40 Gsample/s oscilloscope (Agilent DSO80804B) and downloaded to a computer for offline analysis. We fit the resulting waveform under the assumption that the signal beam has a Gaussian envelope and a phase that is a second-order polynomial. In this case, the quadratic term is directly related to β_2 by $\phi = -\{\beta_2 L / [1 + (\beta_2 L / \tau_0^2)^2]\} t^2 / 2\tau_0^4$. We also fit the data with a fourth-order polynomial and find that the reduced-chi-square is larger than when fitting a quadratic polynomial, indicating that higher-order dispersion has a negligible effect on the GVD-induced chirp.

#210131 - $15.00 USD Received 14 Apr 2014; revised 27 May 2014; accepted 29 May 2014; published 4 Jun 2014

Figure 4(b) shows that β_2 increases linearly with G (proportional to P_{pj}) as expected, demonstrating all-optical control of the GVD. We obtain a maximum value of $|\beta_2|$ = 7.8 ns^2/m, which is ~10^9 times larger than that obtained in standard telecommunication optical fibers at 1.55 μm. Negative GVD can be obtained by inverting Δ (see Fig. 3(b)). Our observations are in good agreement with Eq. (4), which predicts that $\beta_2 = -20.9\,\mathrm{sgn}[\Delta]G$ (ns^2/m) for $|\Delta/\gamma| = 1.03$, where sgn is the sign function. There are no free parameters in our model.

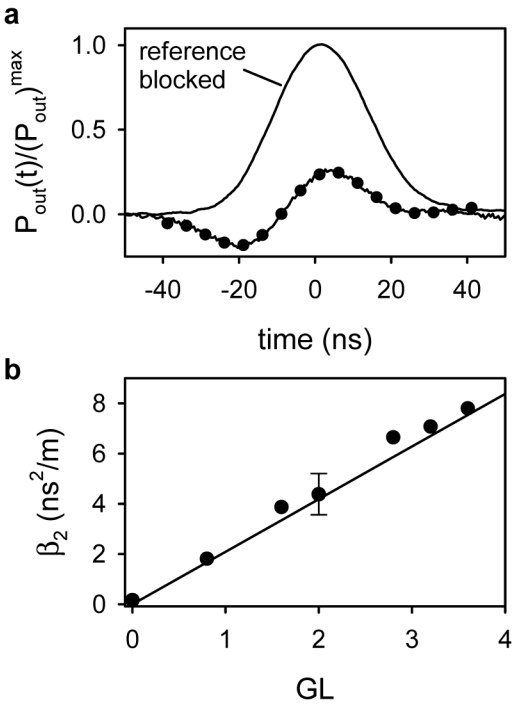

Fig. 4. Observation of giant GVD in a laser-pumped optical fiber. **a** Temporal evolution of the power at the output port $P_{out}(t)$ of the homodyne detection setup normalized to its peak power ($(P_{out})^{max}$) for GL = 2.0 ± 0.08. When the reference beam is blocked (solid line, top), we observe the pulse profile. With the reference beam (solid line, bottom), we observe a complex pattern resulting from both the pulse profile and the temporal phase variation resulting from the GVD-induced chirp. The solid dots are a fit to the data (see text). **b** Linear variation of the GVD parameter with SBS gain, which is proportional to the power of the pump laser. The error bar shows the typical error in our measurement.

4. Discussion of pulse distortion

From the temporal pulse profile measurements shown in Fig. 4(a), we observe that there are some small distortions in the transmitted pulse properties, which are not expected based on our discussion above that assumes an idea transparent dispersive medium for which the imaginary part of β is essentially equal to zero. In an ideal dispersive medium, a chirp-free Gaussian pulse gains a pulse width broadening determined by β_2. In our SBS-based GVD system, however, we have observed small pulse shape distortions including additional broadening, amplification and delay (shown in Fig. 5). These non-ideal effects are due predominantly to frequency-dependent gain and absorption arising from the imaginary part of β, which is unavoidable for a material satisfying the Kramers-Kronig relation [17]. These small non-ideal behaviors do not disrupt the GVD-induced linear frequency chirp and, furthermore, initial simulations show that they can be reduced substantially by tailoring the

#210131 - $15.00 USD Received 14 Apr 2014; revised 27 May 2014; accepted 29 May 2014; published 4 Jun 2014

pump beam spectrum using methods similar to those used to minimize pulse distortion in SBS-based slow- and fast-light [18].

We use two approaches for understanding the origin of the pulse distortion: a numerical solution to Eq. (1) using the full frequency-dependent susceptibility given in Eq. (3), and an approximate analytic method where we truncate the Taylor series expansion given in Eq. (2) after the second-order term. When the carrier frequency of the pulse is at the center of the composite resonance ($\delta = 0$), β_j is pure imaginary for j odd and pure real for j even (ignoring the dispersion of the silica). We assume this resonance condition in the discussion below, where we compare the predictions of the approximate analytic model, the full model, and experimental observations.

The envelope of the pulse field amplitude transmitted through the laser-pumped fiber, assumed to be propagating along the + z-direction and for the case where the entrance face of the medium is at z = 0, can be found analytically for an input Gaussian pulse of the form

$$A(z=0,t) = A_0 \exp\left[-\left(t/\tau_0\right)^2\right]. \tag{4}$$

After substantial calculation, we find the output pulse is Gaussian and that the analytic solution has the expected behavior for a material with GVD, including a frequency chirp and pulse broadening, as well as some non-ideal effects discussed below that arise from the imaginary part of β_1. The predicted pulse broadening, characterized by the Gaussian pulse-width parameter at the output of the dispersive material ($z = L$), is given by

$$\tau^2 = \tau_0^2(1 + L^2 / L_D^2), \tag{5}$$

where $L_D = \tau_0^2 / |\beta_2|$, and is identical to the result found for an ideal GVD material.

One non-ideal effect is a pulling of the pulse carrier frequency due to the frequency-dependent gain (see Fig. 1(b)). The instantaneous pulse carrier frequency is given by

$$\omega(T) = \omega_0 - \frac{\partial \phi}{\partial T}, \tag{6}$$

where $T = t - \mathrm{Re}[\beta_1]z$ is the local time in the frame moving at the group velocity arising from the silica glass (not including the dispersion from the SBS resonances). The time-dependent phase in Eq. (6) is given by

$$-\frac{\partial \phi}{\partial T} = \frac{\mathrm{sgn}(\beta_2)L}{L_D \tau^2} T - \frac{\mathrm{Im}(\beta_1)L}{\tau^2}, \tag{7}$$

where the first term on the right-hand-side of Eq. (8) is the linear chirp expected for a material with GVD and the second term represents the non-ideal frequency shift. Here,

$$\mathrm{Im}(\beta_1) = -\frac{G}{2\gamma}\left[\frac{4\tilde{\Delta}}{\left(1+\tilde{\Delta}^2\right)^2}\right]. \tag{8}$$

For our experiment, the frequency shift is of the order of γ (~$2\pi \times 24$ MHz) for the largest value of G, which can be compensated using an acousto-optic modulator, for example, if required for a specific application.

Another non-ideal effect is that the Gaussian pulse experiences a temporal offset given by

$$T_{off} = -\frac{\mathrm{sgn}(\beta_2)\,\mathrm{Im}(\beta_1)L^2}{L_D}, \tag{9}$$

#210131 - $15.00 USD Received 14 Apr 2014; revised 27 May 2014; accepted 29 May 2014; published 4 Jun 2014

which arises from both the effects of the first- and second-order dispersive terms in Eq. (2).

Finally, the pulse experience an overall amplification so that the ratio of the output to input power is given by

$$\frac{P_{out}}{P_{in}} = \left(\frac{\tau_0}{\tau}\right)^2 \exp\left[\frac{\left(\mathrm{Im}(\beta_1)L\right)^2}{\tau_0^2}\right]. \tag{10}$$

The prefactor in Eq. (10) is the expected result for a medium with pure GVD so that the pulse decreases in amplitude as it broadens. The exponential term arises from the fact that some of the pulse spectrum overlaps with the amplifying part of the composite gain line as its frequency is pulled toward the amplifying side of the resonance.

By direct measurement of the temporal evolution of the pulse at the output of the GVD medium, we determine the pulse width, temporal offset, and amplification as a function of the SBS gain as shown in Fig. 5 and compare to the approximate analytic theory outlined above and the numerical solution using the full susceptibility. It is seen that there is good agreement between the experiments and both theoretical approaches for the pulse offset and amplification. However, the pulse broadens more than expected in the experiment when compared to the second-order theory, but is in good agreement with the full analysis. The additional pulse broadening results from the frequency filtering effect due to third and higher order dispersive terms in Eq. (2). Overall, these effects are small and may not be important for specific applications that mainly require a linear chirp of the input pulse. Also, we reiterate that these effects can be mitigated by tailoring the pump spectrum.

Finally, we comment that that the Taylor series given in Eq. (2) has no radius of convergence when $|\Delta/\gamma| < 1$ and there is substantial disagreement between our approximate analytic expressions and the theory using the full susceptibility. Therefore, we conduct the experiment with $\Delta/\gamma = \pm 1.03$ even though the GVD parameter β_2 takes on its maximum value when $\Delta/\gamma = \pm 0.73$.

5. Conclusion and outlook

In conclusion, we have successfully realized a strongly dispersive material with large tunable group velocity dispersion (GVD) via SBS in a photonic crystal fiber. We have obtained giant and tunable GVD over the range ± 7.8 ns^2/m, verified by the measurement of the quadratic phase chirp induced on a 28-nanosecond-duration pulse. The dispersive properties of the fiber agree well with the theoretical model. Small pulse distortions are accounted for with second-order approximate analytic model and full-rank numerical simulation.

#210131 - $15.00 USD Received 14 Apr 2014; revised 27 May 2014; accepted 29 May 2014; published 4 Jun 2014

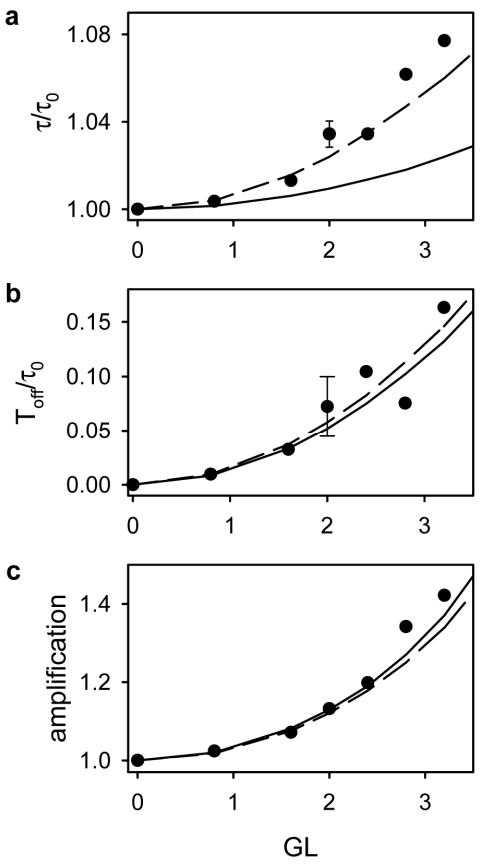

Fig. 5. Parameters for an optical pulse propagating through a dual-line dispersive material. a Pulse width, b temporal offset, and c amplification as a function of the SBS gain. Here, amplification is defined at the peak power of the output probe pulse divided by the peak power of the pulse in the absence of the pump beams (*i.e.*, with $G = 0$). The solid lines are the prediction of the second-order theory, the dashed lines are the predication of the full model using numerical techniques, and the solid circles are the experimental measurements, where the error bars indicate typical measurement error. In **c**, the typical error bar is of the order of the size of the symbol.

There are many possible future directions of the work presented here that will allow for complete control of GVD in optical materials over a wide range of pulse parameters. For the SBS-based GVD investigated here, the resonances can be broadened to the 10's of GHz range by tailoring the pump spectrum [19,20], thereby realizing large GVD for pulses from the nanosecond to the sub-100-ps range. Also, there is sustained progress in realizing chip-scale SBS-based devices [21–23], which will allow compact dispersive GVD systems. In the quantum regime, it will be possible to disperse single-photon wavepackets without adding excess noise [24] if the SBS device is cooled to its quantum mechanical ground state, which is now within reach [25]. Considering other platforms, recoil-induced resonances in laser-pumped ultra-cold gases [26] should display large GVD for millisecond-scale pulses and Fano-type resonances in photonic crystal [27], plasmonic [28] and metamaterial [29] devices are promising avenues to explore for high-bandwidth GVD engineering.

Acknowledgments

We gratefully acknowledge the financial support of the DARPA DSO InPho program and the U.S. Army Research Office MURI award W911-NS-09-10406.

#210131 - $15.00 USD Received 14 Apr 2014; revised 27 May 2014; accepted 29 May 2014; published 4 Jun 2014